

See discussions, stats, and author profiles for this publication at: <https://www.researchgate.net/publication/23404044>

# Physicochemical Determinants of Multiwalled Carbon Nanotube Bacterial Cytotoxicity

ARTICLE *in* ENVIRONMENTAL SCIENCE AND TECHNOLOGY · NOVEMBER 2008

Impact Factor: 5.33 · DOI: 10.1021/es8010173 · Source: PubMed

---

CITATIONS

160

READS

96

## 3 AUTHORS, INCLUDING:



Seoktae Kang

Kyung Hee University

53 PUBLICATIONS 2,861 CITATIONS

[SEE PROFILE](#)



Menachem Elimelech

Yale University

394 PUBLICATIONS 32,496 CITATIONS

[SEE PROFILE](#)

# Physicochemical Determinants of Multiwalled Carbon Nanotube Bacterial Cytotoxicity

SEOKTAE KANG, MEAGAN S. MAUTER,  
AND MENACHEM ELIMELECH\*

Department of Chemical Engineering, Environmental  
Engineering Program, Yale University,  
New Haven, Connecticut 06520-8286

Received April 11, 2008. Revised manuscript received May 20, 2008. Accepted June 17, 2008.

Rational modification of carbon nanotubes (CNTs) to isolate their specific physical and chemical properties will inform a mechanistic understanding of observed CNT toxicity in bacterial systems. The present study compares the toxicity of commercially obtained multiwalled carbon nanotubes (MWNTs) before and after physicochemical modification via common purification and functionalization routes, including dry oxidation, acid treatment, functionalization, and annealing. Experimental results support a correlation between bacterial cytotoxicity and physicochemical properties that enhance MWNT-cell contact opportunities. For example, we observe higher toxicity when the nanotubes are uncapped, debundled, short, and dispersed in solution. These conclusions demonstrate that physicochemical modifications of MWNTs alter their cytotoxicity in bacterial systems and underline the need for careful documentation of physical and chemical characteristics when reporting the toxicity of carbon-based nanomaterials.

## Introduction

Carbon nanotubes (CNTs) are now widely used in commercial applications. While single-walled nanotubes (SWNTs) are hailed for specific electronic, optical, or chemical attributes present on the individual nanotube scale, the unique properties of multiwalled carbon nanotubes (MWNTs) are generally associated with the bulk material. Aggregate properties of MWNTs such as high surface area, thermal conductivity, or tensile strength are further tailored for specific applications through postsynthesis chemical and thermal modification procedures (1). Annealing, for instance, reduces structural defects and removes catalytic metals used in synthesis (2). Functionalization with strong oxidizing agents improves dispersivity in aqueous solutions and enhances compatibility with composite matrix materials (3).

This commercial focus on tailored manipulation of MWNTs' bulk properties should influence the interpretation of studies revealing MWNTs' impacts on human health or the environment. First, bulk applications demand large quantities of nanomaterials; MWNT release into the environment may soon constitute a substantial material flow. Second, the tailored adaptation required for many bulk applications of MWNTs implies significant physicochemical variation between the released nanotubes. Finally, the commercial emphasis on bulk properties diminishes the

necessity for MWNT samples with high purity and precise reproducibility.

The diversity of MWNT samples utilized for commercial application complicates attempts to identify and reduce human and environmental implications. Past toxicity assessments have differentiated between single-walled and multiwalled nanotubes (4–8), but only a few have investigated the effects of physicochemical modification (9–12). Tian et al. (11) explored the eukaryotic cytotoxicity of a wide range of nanoscale carbonaceous materials, including SWNTs, activated carbon, carbon black, MWNTs, and carbon graphite. Their conclusions support surface area and surface chemistry as primary determinants of toxicity. Sayes et al. (10) performed *in vitro* cytotoxicity screens on cultured human dermal fibroblasts to elucidate the effects of varying degrees of carboxylic acid functionalization on SWNTs. Unfortunately, these studies were never expanded to include alternative modification routes or probe the cytotoxicity of alternative classes of CNTs, such as MWNTs. Furthermore, functionalization simultaneously modifies dispersivity in solution and CNT length, thereby challenging researchers' ability to differentiate the effects of surface chemistry from aggregation state and physical properties (11, 12). At this writing, no toxicological study on bacteria has provided detailed characterization of physical and chemical properties of a single class of sequentially modified carbon-based nanomaterials to support toxicity results.

The omission of physicochemical characterization data also complicates efforts to compare toxicity results between research studies. Meta-analyses of carbon nanomaterial toxicity draw upon studies with vastly different solution chemistry, sample purity, synthesis technique, and nanomaterial manufacturer (4, 5, 7, 8). The nanomaterials were often poorly characterized prior to experimentation, and the toxicity results provide little direction for green applications or green design of carbon-based nanomaterials.

Given the expense and complexity of assessing toxicity for each possible MWNT sample modification, general correlations between cytotoxicity and physicochemical properties of nanotubes will be fundamental to low-risk commercial applications of nanomaterials. These correlations will require simultaneous material characterization and standardized toxicity assays. Carefully documented and well-defined studies will also inform a mechanistic understanding of nanomaterial toxicity.

The present study initiates the transition toward toxicity assessment techniques that incorporate rational physical or chemical modifications to elucidate a mechanistic understanding of MWNT toxicity in *Escherichia coli*. A compound's bacterial toxicity is both an indicator for adverse effects toward the diverse ecological and environmental functions served by single-cell organisms, as well as an initial screen for potential eukaryotic toxicity. We compare commercially obtained MWNTs to nanotube samples modified under common purification and functionalization routes, including dry oxidation, acid treatment, functionalization, and annealing. Each of the samples is derived from the same initial bulk MWNT stock to reduce variability in sample purity. Though these results cannot be extrapolated to toxicity in nonbacterial models, careful correlation between physicochemical properties and cytotoxic observations will inform mechanistic pathways of MWNT toxicity in bacterial systems.

Our results indicate that common purification and functionalization procedures significantly alter the physical and chemical properties of MWNTs. These physicochemical modifications also have a direct impact on the cytotoxicity

\* Corresponding author phone: (203) 432-2789; e-mail: menachem.elimelech@yale.edu.

of MWNT samples in *E. coli* K12. While our investigation lacks the comprehensive scope necessary to establish direct links between physicochemical properties and bacterial cytotoxicity, we do note that biotoxicity increases in MWNTs that are uncapped, short, functionalized, and form disperse suspensions in aqueous solution.

## Materials and Methods

**Preparation of MWNTs.** The spectrum of MWNTs prepared for this research originate from the successive modification and purification procedures outlined in Supporting Information (Figure S1). As prepared MWNTs (AP-MWNTs) were purchased from NanoTechLabs Inc. (Yadkinville, NC). AP-MWNTs were synthesized via chemical vapor deposition with iron nanoparticle catalysts. AP-MWNTs were dry oxidized in air at 350 °C for 6 h (DO-MWNTs) to remove amorphous carbon species. Subsequent reflux of DO-MWNTs in a 10 M HCl solution at 70 °C for 18 h reduced catalytic metal contamination to yield acid treated MWNTs (AT-MWNT). AT-MWNTs are functionalized (f-MWNTs) via sonication in a mixture of H<sub>2</sub>SO<sub>4</sub> and HNO<sub>3</sub> (3:1 v/v) for 1 h at room temperature (22 °C). Following acid treatment, the carbon products were washed with excess deionized water until the MWNT suspension reached a pH of 6 and collected on an Omnipore membrane (Millipore, U.S.) filter. In parallel, AP-MWNTs were placed at 2000 °C for 12 h in argon to remove catalytic metal and anneal the structural imperfections (AN-MWNTs). The short MWNTs (s-MWNTs) were prepared by annealing as-prepared short MWNTs provided by CEA-CNRS (Gif sur Yvette, France). Prior to use, all MWNTs were dispersed in an aqueous saline solution (0.9% or 0.154 M NaCl) and sonicated for 15 min (Aquasonic 150T, VWR, U.S.).

**Characterization of MWNTs.** Characterization of as-prepared and modified MWNTs included Raman spectroscopy, transmission electron microscopy (TEM), and scanning electron microscopy (SEM) techniques. A Raman spectrometer (Jobin Yvon, Japan) equipped with an Olympus confocal microscope (Olympus Corporation, Japan) recorded Raman spectra for MWNTs after excitation at 532 nm. The ratio of G-band (1579 cm<sup>-1</sup>) to D-band (1349 cm<sup>-1</sup>) peaks in the Raman spectra of MWNTs provided a qualitative indicator for comparing the structural imperfections and the content of inert matter in the nanotube sample (13). Additional MWNT characterization involved TEM imaging, thermogravimetric analysis (TGA), energy dispersive X-ray spectroscopy (EDX), and SEM (details in the Supporting Information).

**Preparation of *E. coli* Cells.** We selected *Escherichia coli* K12 as the model organism for cytotoxicity experiments for consistency with our recent studies (14, 15). *E. coli* K12 were grown in LB medium at 37 °C and harvested at midexponential growth phase. Cells were washed twice and resuspended in saline solution (0.9% or 0.154 M NaCl) before exposure to the MWNT samples.

**Bacterial Toxicity Assays.** Conclusive toxicity studies include assays for both cell membrane integrity and cell metabolic activity. To facilitate direct contact between the nanotube samples and the bacteria, we employed the CNT-coated filter method described in our previous study (15). Filtration preparation consisted of dispersing 4 mg of MWNTs in 10 mL of dimethyl sulfoxide (DMSO) and sonicating the solution for 15 min. Filtering the suspension through a 5 μm PVDF membrane (Millipore) formed MWNT-coated filters on top of the PVDF membrane. Washing the filter with 100 mL of ethanol removed residual DMSO, and a final rinse with 200 mL deionized water removed any remaining ethanol. Filters were prepared for each of the six MWNT samples.

After filter preparation, we filtered 50 mL of 0.9% (0.154 M) NaCl saline solution with 2 × 10<sup>6</sup> *E. coli* cells through either the MWNT-coated filter or a bare 0.45 μm PVDF

membrane filter (serving as a control). The membrane coupons were then incubated for 30 min in the saline solution at 37 °C, after which cell viability was assessed.

We evaluated cell membrane integrity using a standard, fluorescence-based, nucleic acid assay. *E. coli* cells were stained with propidium iodide (PI, 50 μM) for 15 min, and counter-stained with 4'-6-diamidino-2-phenylindole (DAPI, 4 μg/mL) for 5 min in the dark. The filter was imaged under an epifluorescence microscope (Olympus) with a U filter (364/440 nm) for detecting cells stained with both PI and DAPI, and an IB filter (464/604 nm) for detecting cells stained with PI. Ten representative images from different locations on each filter were captured for subsequent data analysis through direct counting methods. The percentage of inactivated cells was determined by the ratio of cells stained with PI to those stained with DAPI plus PI.

We verified the cell viability obtained in our membrane damage assays using a parallel test for cell metabolic activity (with 5-cyano-2,3-ditoly-tetrazolium chloride, CTC). Details are given in our recent publications (14, 15) and in the Supporting Information.

**Efflux of Intracellular Matters.** The efflux of genomic material provides a final verification of compromised cell viability. Plasmid DNA (p-DNA) and RNA served as markers for the efflux of intracellular material, though p-DNA's resistance to degradation suggests that it is a more robust assay. In contrast with the fluorescence based DAPI/PI and CTC assays using a deposited MWNT exposure method, the efflux assays assessed toxicity using the suspended CNT method described in Kang et al. (15). This suspended method enables solution phase purification and quantification of intracellular material. Previous results demonstrate no significant difference in toxicity between the suspended and deposited methods (15).

We compared the solution concentrations of p-DNA in bacterial suspensions incubated with 20 μg/mL dispersed MWNTs against cells without MWNTs. Large MWNT aggregates formed during the incubation, and bacterial cells attached to the exposed surface of the MWNT aggregates, as was observed in our recent bacterial toxicity work with SWNTs (15). Plasmid vector pGEM-Teasy (3015 bp) was electroporated into *E. coli* XL1 blue (16). As above, the strain was harvested at exponential growth phase, washed and resuspended in 0.9% (0.154 M) NaCl solution, and incubated in the presence of different MWNT samples (20 μg/mL) for 60 min. After centrifugation and filtration through a 0.22 μm low protein binding Millex membrane (Millipore), the concentration of plasmid DNA in the filtrate was analyzed by an ND 1000 spectrophotometer (NanoDrop, U.S.) and the purity of p-DNA was evaluated by the ratio of UV absorbance at 260–230 nm (>1.8). For each condition, the solution concentration of p-DNA was corrected to account for the amount of p-DNA that adsorbed to the suspended MWNTs (SI). In addition to p-DNA, we quantified the efflux of intracellular RNA. Details on cell incubation with MWNTs and the RNA purification and quantification protocols are given in the Supporting Information.

**Direct Imaging of *E. coli* Cells on MWNT-Coated Filters.** We performed SEM to verify cytotoxicity and investigate cell morphology on the MWNT-coated filters. Filters were first incubated for 30 min in 0.9% (0.154 M) NaCl solution and subsequently fixed with glutaraldehyde and osmium tetroxide for SEM imaging (17).

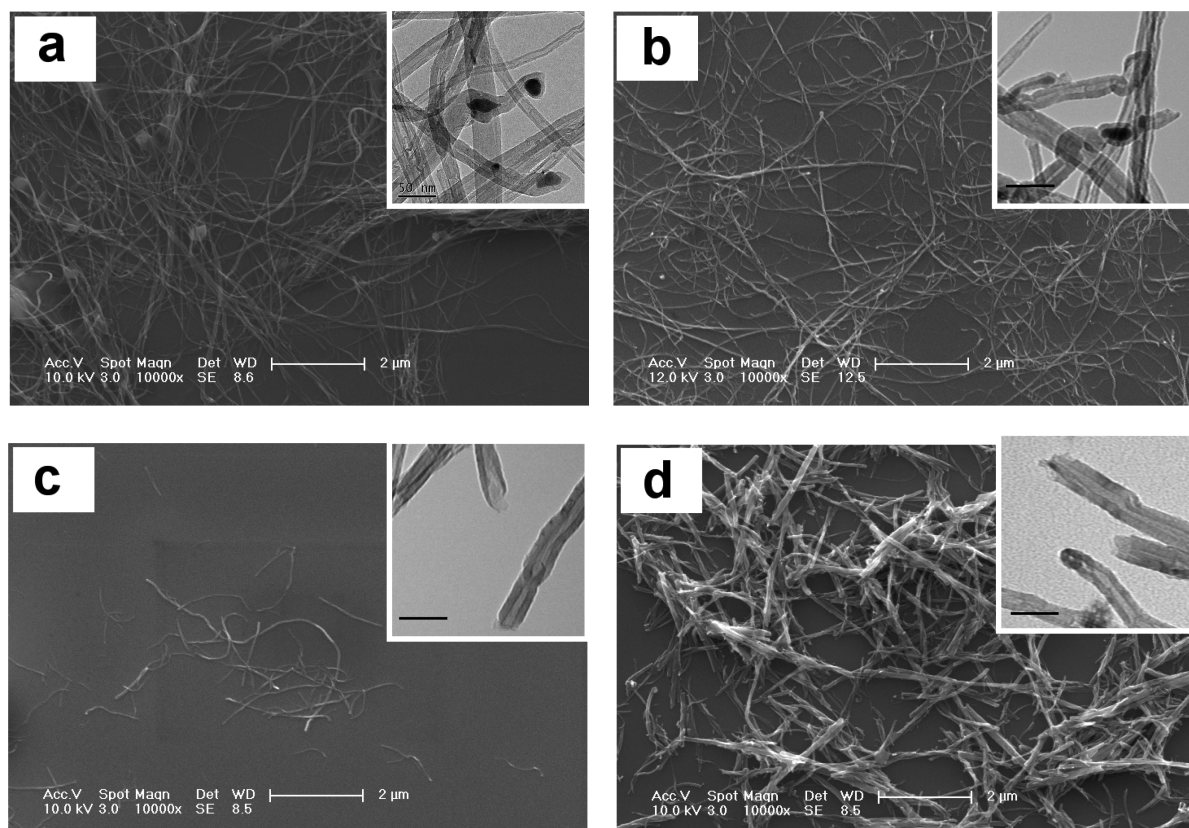
## Results and Discussion

**Physicochemical Properties of MWNT Samples.** Detailed characterization of the modified MWNT samples informs potential links between physicochemical properties and bacterial cytotoxicity. Properties with suspected relevance to both commercial application and cytotoxicity include

**TABLE 1. Physicochemical Properties and Bacterial Toxicity of MWNT Samples**

	physical properties			chemical properties		E. coli toxicity
	diameter <sup>a</sup> (nm)	length <sup>a</sup> ( $\mu\text{m}$ )	aspect ratio	RM <sup>b</sup> (%)	G/D <sup>c</sup>	% inactivated cells <sup>d</sup>
AP-MWNT	17 $\pm$ 9	91 $\pm$ 21	5300	6.7	1.47	13.6 $\pm$ 3.1
DO-MWNT	20 $\pm$ 8	84 $\pm$ 18	4200	4.6	1.95	10.4 $\pm$ 2.4
AT-MWNT	17 $\pm$ 6	77 $\pm$ 31	4500	2.1	2.47	32.7 $\pm$ 4.2 <sup>e</sup>
f-MWNT	19 $\pm$ 7	4.1 $\pm$ 3.7	220	3.7	1.11	41.6 $\pm$ 3.7 <sup>e</sup>
AN-MWNT	21 $\pm$ 11	82 $\pm$ 23	3900	0.8	3.72	26.3 $\pm$ 7.9 <sup>e</sup>
s-MWNT	35 $\pm$ 20	2.3 $\pm$ 0.6	66	0.7	4.15	28.7 $\pm$ 3.8 <sup>e</sup>

<sup>a</sup> Average diameters and lengths of AP-MWNT, DO-MWNT, AT-MWNT, and AN-MWNT were determined by TEM and SEM images, respectively ( $n = 10$ ). For f-MWNT and s-MWNT, 50 tubes were averaged from five TEM images. <sup>b</sup> Residual mass (%) after thermo-gravimetric analysis (TGA). EDX analysis showed that most of TGA residues in all MWNT samples were iron oxides (data not shown). <sup>c</sup> The ratio of Raman G-band ( $\sim 1580 \text{ cm}^{-1}$ ) to D-band ( $\sim 1350 \text{ cm}^{-1}$ ) peak height at  $\lambda_{\text{laser}} = 532 \text{ nm}$ . <sup>d</sup> Based on fluorescence-based toxicity test (Supporting Information Figure S5a) and subsequent statistical analysis. The cell inactivation for the control (0.45  $\mu\text{m}$  PVDF membrane filter without MWNTs) was 7.5  $\pm$  2%. <sup>e</sup> Sample toxicity statistically different from control at a 95% confidence level ( $p$ -value  $< 0.05$ ). Details on the statistical analysis are given in the SI.

**FIGURE 1. SEM and TEM (inset) micrographs of MWNT samples: (a) AP-MWNT, (b) AT-MWNT, (c) f-MWNT, and (d) s-MWNT. The bars in the SEM and TEM images represent 2  $\mu\text{m}$  and 50 nm, respectively.**

diameter, length, aspect ratio (length/diameter), sample purity tabulated as residual mass after thermogravimetric analysis, and the structural defects in the nanotube sample indexed by the G-band to D-band ratio of the Raman spectra. The results of TEM, SEM, and Raman spectra analysis are summarized in Table 1. The corresponding bacterial toxicity values presented in Table 1 will be discussed in a subsequent section of this paper.

Functionalization and purification procedures alter the physicochemical properties of MWNTs significantly enough to change MWNT cytotoxicity in *E. coli*. The first purification step from AP-MWNTs to DO-MWNTs removed amorphous carbon, as demonstrated by an increase in the Raman spectrum G/D ratio (Table 1). The subsequent acid treatment of DO-MWNTs effectively removed catalytic metal contamination and reduced total metal (oxide) content of the AT-

MWNTs to a residual mass of 2.1% (Table 1). The size and aspect ratios of the MWNT samples were not affected by the purification sequence yielding AT-MWNTs.

The removal of amorphous carbon and catalytic metals is confirmed in the SEM images and TEM insets provided in Figure 1. The reduction in unstructured carbon particles between the SEM images of AP-MWNTs and AT-MWNTs, as well as the disappearance of black (light adsorbing) metal clusters in the TEM micrograph of AT-MWNTs, verify successful purification.

Modification with an array of covalently bound functional groups enables tailored manipulation of the nanotubes' chemical properties. While nanotube functionalization chemistry has become an expansive field, the majority of covalent modifications begin with the introduction of carboxylic and hydroxyl groups on the tips and sidewalls of the carbon

nanotubes. These polar functional groups enhance the dispersivity of the MWNTs (SI Figure S2), thus expanding pathways for derivitization (1, 3).

The harsh chemical conditions necessary for introducing functional groups also affect the physical properties by cleaving the nanotubes and introducing structural defects. The mean length of the large bundles dropped from 77 to 4.1  $\mu\text{m}$  following a standard functionalization procedure of sonication in a mixture of  $\text{H}_2\text{SO}_4$  and  $\text{HNO}_3$  (Table 1, Figure 1). As expected, the introduction of functional groups also reduced the G/D ratio of the sample (Table 1) (13).

Annealing at high temperature in the absence of oxygen is also effective in removing residual metal contamination. The residual masses of AN-MWNTs and s-MWNTs in thermo-gravimetric analysis are 0.8% and 0.7%, respectively (Table 1, SI Figure S3). TEM imaging (representative micrograph presented in Figure 1) confirms the absence of catalytic metal aggregates. In addition to removing contaminants, the high temperature annealing process reduces structural imperfections in the sample (2, 18). The thermodynamically favorable conformation of defect-free nanotubes over those with Stone-Waals arrangements or holes in the sidewalls is achieved through controlled heating and cooling of the nanotube samples in an anoxic environment. This high degree of structural order is revealed in the large G/D ratios of 3.72 for AN-MWNTs and 4.15 for s-MWNTs (Table 1), as well as in the higher thermal resistances (SI Figure S3).

**Bacterial Toxicity of MWNT Samples.** Variations upon the physical, chemical, and structural properties of MWNTs are fundamental to their commercial application. This research aimed to characterize the physical and chemical origins of MWNT cytotoxicity in *E. coli* by correlating precisely measured properties to quantitative indicators of bacterial toxicity. The six MWNT samples were modified according to routes that decoupled key physicochemical and structural properties, including length, catalytic metal content, aggregation state, and surface chemistry. Our results confirmed previous reports (4, 5, 14) that MWNTs exhibit moderate antimicrobial activity. Pretreatment, purification, and functionalization modifications that alter the physicochemical properties of the MWNT samples have a relatively modest effect on bacterial toxicity.

The bacterial toxicity of AP-MWNTs and DO-MWNTs was not statistically significant at 95% confidence when compared to control experiments on a bare 0.45  $\mu\text{m}$  PVDF membrane filter, likely due to the small sample size (three samples) of the membrane damage assay. DAPI/PI staining, an indicator of cell membrane damage, revealed AP-MWNT and DO-MWNT sample toxicity rates below 14 and 10%, respectively (Table 1, SI Figure S5a). Metabolic activity tests confirmed the minimal cytotoxic effects (SI Figure S5b), though this assay is less sensitive to toxicity than the DAPI/PI staining method. Comparison between the AP-MWNT and DO-MWNT samples suggests that amorphous carbon does not appreciably affect cytotoxicity in *E. coli*.

Catalytic metal (Fe) content in the MWNT samples did not correlate to cell membrane damage. Indeed, AT-MWNTs, with a residual mass content 50–70% lower than the DO-MWNT and AP-MWNTs, exhibited significantly higher toxicity in both cell membrane integrity and metabolic activity assays. AN-MWNTs, which have catalytic metal contents of nearly zero, exhibited higher toxicity than DO-MWNTs that contain moderate levels of Fe.

Cytotoxicity results from the remaining MWNT samples reveal moderate losses to membrane integrity and reductions in metabolic activity when compared to control experiments (Table 1, SI Figure S5b). Membrane integrity assays assign toxicity values in the range between 26 and 33% for the AT-, AN-, and s-MWNT samples (Table 1). Functionalized MWNTs

exhibited the highest rates of cytotoxicity with nearly 42% of the *E. coli* cells stained by PI.

Though the quantitative analysis of physical and chemical properties outlined in Table 1 informs possible links between MWNT properties and bacterial cytotoxicity, these properties do not capture the aggregation state or dispersivity of the nanomaterials in an aqueous environment. We hypothesize that nanotube-cell membrane interactions are affected by the dispersivity and conformation of the nanotube bundles. Functionalization of the sidewalls with polar functional groups simultaneously enhances nanotube dispersivity in polar solvents and reduces nanotube bundling. The shortened, functionalized nanotubes of the f-MWNT sample were significantly more disperse than other MWNT suspensions. The s-MWNT sample was the second most disperse sample (SI Figure S2), despite the high bundling of the nanotubes shown in the SEM micrograph (Figure 1d).

Qualitative observations of dispersivity (SI Figure S2) and aggregate morphology (Figure 1) suggest a possible correlation between dispersed nanotubes and elevated cytotoxicity (Table 2). We use dispersion in aqueous solution to approximate the MWNTs' hydrophilicity and morphology when deposited on the filter. SEM images of the f-MWNT sample revealed short and debundled nanotubes, while dispersivity observations indicate that the sample is well dispersed in aqueous solutions and relatively hydrophilic due to the presence of polar functional groups. The s-MWNTs are also somewhat disperse in aqueous solutions due to their smaller size (SI Figure S2), but they adopt a highly bundled morphology in SEM images (Figure 1). We suggest that the elevated toxicity of dispersed and debundled nanotubes may stem from increased contact opportunities with the cells, though we acknowledge that these aqueous phase properties are inseparable from other physical and chemical properties such as length, surface area, functional groups, hydrophobicity, or aggregation state.

**Efflux of Intracellular Matter.** The present study assessed bacterial toxicity through assays for metabolic disturbance and membrane damage (15). While membrane damage assays are a strong surrogate for cell death, it is possible for bacteria to repair moderately damaged cell membranes (19). Thus, we sought to verify membrane damage rates obtained via a fluorescent staining method with a secondary assay targeting complete cell membrane damage. The efflux of large quantities of intracellular matter in cells occurs when cells have suffered irreparable damage to their cell walls and inner membranes.

While the intracellular matter efflux assay is effective in comparing relative degrees of cellular membrane damage among the different MWNT samples, the assay suffers two key drawbacks. The first limitation originates from the difficulty in relating the dependent variable of the p-DNA concentration back to a percentage of lysed cells. The second limitation is that nucleic acids display strong sorption affinities for carbon nanotubes (20). To overcome this second limitation, we corrected the concentration of p-DNA in solution by accounting for the amount adsorbed on MWNTs after one hour of equilibration time in the presence of purified plasmid DNA.

Despite these limitations, results from efflux assays verify that f-MWNTs and s-MWNTs are associated with higher potential damage to cellular membranes (Figure 2). In the p-DNA assay, *E. coli* incubation with f-MWNTs increased the concentration of p-DNA in the supernatant over the other MWNT samples. Consistent with the fluorescence-based toxicity assay, incubation with s-MWNTs conferred the second highest release of the intracellular matter. The remaining MWNT samples did not differ significantly from one another. This is again consistent with the lower rates of

**TABLE 2. Qualitative Comparison of Bacterial Toxicity with Various Physical and Chemical Properties of MWNTs<sup>a</sup>**

Toxicity Classification <sup>b</sup>	Low-range	Mid-range			Upper-range
Amorphous Carbon Present <sup>c</sup>		✓			
Uncapped <sup>d</sup>		✓	✓	✓	✓
Debundled <sup>e</sup>			✓		✓
Short Length <sup>f</sup>				✓	✓
Dispersed in Solution <sup>g</sup>				✓	✓
	DO-MWNT	AP-MWNT	AN-MWNT	AT-MWNT	s-MWNT
					f-MWNT

<sup>a</sup> The data presented is binned into yes (checked) or no (blank) to qualitatively reflect individual sample properties in comparison to the other MWNT samples. <sup>b</sup> Toxicity classification is a qualitative representation of the degree of bacterial cytotoxicity as observed from the membrane damage assay (Table 1 and SI Figure S5a), metabolic activity test (SI Figure S5a), and cellular matter efflux assays (Figure 2 and SI Figure S6). <sup>c</sup> Indicated by TGA and SEM images. <sup>d</sup> Indicated by TEM and SEM images., <sup>e</sup> Indicated by TEM and SEM images. <sup>f</sup> Indicated by SEM images. <sup>g</sup> Indicated by qualitative settling experiment (SI Figure S2).

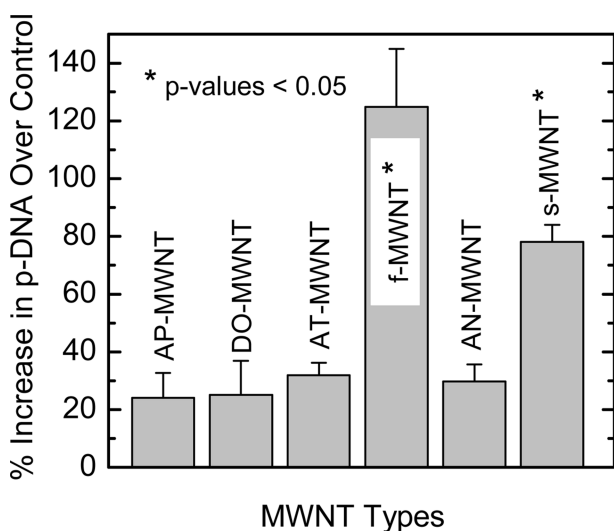


**FIGURE 2. Corrected plasmid DNA (p-DNA) concentration in the supernatant following *E. coli* incubation with MWNT samples.** Washed and resuspended *E. coli* cells ( $5 \times 10^6$ /mL) were incubated for 1 h in 20 mL of 0.9% (0.154 M) NaCl solution with 20  $\mu\text{g}$ -MWNTs/mL. The p-DNA concentration for the control (suspended cells with no MWNTs) was 3.5  $\mu\text{g}/\text{mL}$ . The asterisks (\*) indicate statistical significance of MWNT samples at a 95% confidence level ( $p$ -value <0.05). Details on the statistical analysis are provided in the Supporting Information.

cell membrane damage measured in the fluorescence-based toxicity assay.

The quantification of RNA efflux from compromised cells is complicated by rapid degradation of RNA at room temperature. This degradation hinders the development of RNA adsorption isotherms necessary for normalizing data across MWNTs with different binding affinities. Thus, low concentrations of RNA in the supernatant may be a function of either low cell lysis rates or high affinity to the carbon nanotubes. Despite these drawbacks, RNA supernatant concentration assays support earlier conclusions that f-MWNTs are the most cytotoxic sample (SI Figure S5).

**Morphological Change of Bacteria in Contact with MWNTs.** Cell membrane damage and intracellular material assays both imply morphological change to the *E. coli* upon exposure to the MWNT samples. SEM imaging of bacteria on the MWNT filters in Figure 3 confirms cell membrane disruption and lysis. SEM micrographs also reveal differences in nanotube structure between the f-MWNT filter and the s-MWNT filter, providing insight into the physicochemical properties relevant to nanotube toxicity in each sample.

The f-MWNTs appear as highly debundled, individual nanotubes in the micrograph of the MWNT deposit layer (Figure 3a). Some *E. coli* cells are flattened or misshapen, while others maintain normal cell physiology. The micrograph suggests that bacteria are captured within the top portion of the MWNT deposit layer, rather than being sieved out at the nanotube–fluid interface. We hypothesize that the dispersivity of f-MWNTs results in a filter morphology that is looser and more diffuse under the aqueous conditions during sample preparation and incubation. Loose morphology enhances the likelihood that cells permeate the upper layer of deposited MWNTs before becoming trapped in subsequent layers of the filter. The debundled and disaggregated conformation of the f-MWNTs may increase contact opportunities between the bacteria and the nanotubes, thereby increasing the apparent toxicity evidenced in the membrane integrity, metabolic activity, and cellular efflux assays.

This looser morphology of the f-MWNT coated filter contrasts sharply with the tightly bundled structure of the s-MWNT coated filter in Figure 3b. In this micrograph, we observe a strong sieving effect with no cell permeation into the MWNT deposit layer. We suspect that the hydrophobic character of the s-MWNTs encourages distinct stratification at the nanotube–fluid interface. The image also verifies the complete cell rupturing hypothesis upon which we developed the p-DNA (and RNA) efflux assays.

**Relating Physicochemical Characteristics to Observed Toxicity.** An alternative interpretation of the MWNT-filter micrograph results could suggest that the cytotoxic effects of MWNTs in bacteria are not a function of a single mechanism, but rather depend on a number of factors, including amorphous carbon content, catalytic metal content, bundled conformation, length, and dispersivity in aqueous

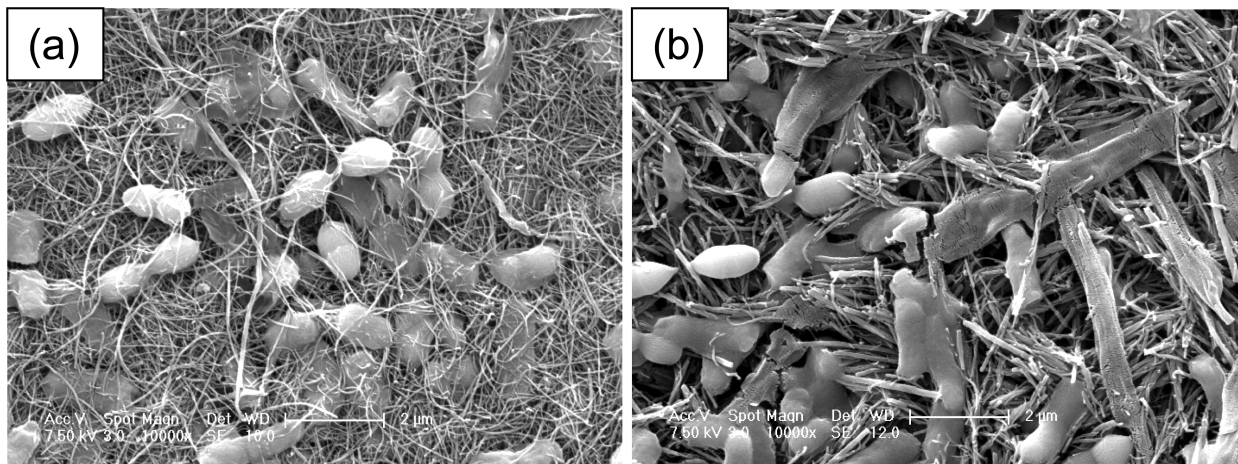


**FIGURE 3.** SEM morphology of *E. coli* cells on (a) f-MWNT and (b) s-MWNT coated filters. Cells on the MWNT-coated filter were first incubated for 30 min in 0.9% (0.154 M) NaCl solution, and then fixed with glutaraldehyde and osmium tetroxide for SEM imaging. The bar in the images represents 2  $\mu$ m.

environments. Table 2 summarizes results from each of the toxicity assays and relates them to these key physicochemical characteristics.

The data presented in Table 2 is binned into categories of yes (checked) or no (blank) to qualitatively reflect individual sample properties in comparison to the other MWNT samples. Toxicity classification in the table is a qualitative representation of bacterial cytotoxicity as observed from the membrane damage assay or percent of PI-stained cells (Table 1 and SI Figure S5a), metabolic activity test (SI Figure S5b), and cellular matter efflux assays (Figure 2 and SI Figure S6). Because this table is intended as a qualitative summary, the reader is referred to previous tables and figures for quantitative values describing physicochemical properties and toxicity. As a whole, Table 2 supports the conclusion that nanotube conformations that promote physical contact with the bacterial cells increase the cytotoxic effects of MWNTs.

The presence of amorphous carbon does not significantly affect the toxicity of MWNT samples in our study. Comparison of the DO-MWNT and AP-MWNT samples supports this conclusion. Furthermore, the SEM and TGA data suggest that amorphous carbon nanoparticles are at relatively low concentrations in the AP-MWNT sample.

In contrast to previous studies implicating catalytic metal residues in the toxicity of unpurified CNTs (21, 22), we observed no correlation between residual metal content and toxicity. AN-MWNTs, which have catalytic metal contents of nearly zero, exhibited slightly higher toxicity than DO-MWNTs containing moderate levels of Fe. The apparent inconsistency between our data and previous studies correlating residual catalytic metal in unpurified SWNTs to elevated toxicity in human epidermal keratinocytes (21) may stem from the relatively low initial metal content of our sample (7%, compared to 30% in the Shvedova et al. (21) study) or an alternate physicochemical modification simultaneously induced during acid treatment. Alternatively, residual catalytic metals may damage eukaryotic cell lines through pathways not affected in bacterial models.

Comparison between the AN-MWNTs and the AT-MWNTs suggests that the bulk conformation of the nanotubes may contribute to sample toxicity. AN-MWNTs adopt a highly bundled conformation and display lower toxicity rates than the debundled AT-MWNTs (Figure 1). The debundled conformation observed in SEM micrographs increases the frequency of contact opportunities between the nanotubes and the cells and may contribute to the higher levels of toxicity observed in DAPI/PI staining.

Short length also corresponds to increased toxicity in our study. Both of the samples with shorter nanotubes displayed higher toxicity in the assay measuring the cellular membrane integrity and efflux of intracellular materials. However, the s-MWNTs did not display significantly higher toxicity than longer AN-MWNTs prepared via the same annealing method. This suggests that though a correlation exists between length and toxicity, length is not necessarily a determining factor in cytotoxicity.

Instead, we suggest that short nanotube lengths contribute to toxicity through the secondary characteristic of dispersion in solution. SI Figure S2, which qualitatively compares the dispersion and stability of MWNT samples in an isotonic solution of 0.9% (0.154 M) NaCl, indicates that s-MWNTs are somewhat more disperse and more stable in solution than other nanotubes with longer lengths. The f-MWNTs, which consistently display the highest rates of cytotoxicity, are well dispersed and very stable in solution. We hypothesize that dispersion in solution may be a strong determinant of toxicity because higher dispersion leads to the formation of MWNT deposit layers that have increased contact opportunities with bacterial cells.

Experimental results support a correlation between cytotoxicity and physicochemical characteristics shared by nanotubes which are uncapped, debundled, short, and dispersed in solution. Nevertheless, we acknowledge that our experimental design cannot explicitly decouple the effects of surface chemistry (i.e., functionalization) from physical characteristics such as short length or debundled conformations.

**Implications.** The data from this study supports the hypothesis that physicochemical modifications of MWNTs alter their cytotoxicity in bacterial systems. This conclusion underlines the need for careful documentation of physical and chemical characteristics when reporting the toxicity of carbon-based nanomaterials. Correlation between bacterial cytotoxicity and physicochemical properties that enhance contact opportunities with cells is also consistent with previous studies indicating that physical contact is a prerequisite for bacterial toxicity. The identification of specific physicochemical properties governing CNT toxicity presents the opportunity for nanomaterial designs or applications that reduce human and environmental impacts.

## Acknowledgments

We acknowledge the support of the National Science Foundation under Research Grant BES-0646247 and BES-

0504258. M.S.M. acknowledges generous support from the NSF Graduate Research Fellowship Program (GRFP) and the EPA Science to Achieve Results (STAR) Graduate Fellowship Program. We are grateful for the assistance of Mathieu Pinault and Codruta Zoican in preparing nanotube samples, and Maggie Montgomery for the statistical analysis.

### Supporting Information Available

Preparation protocol for MWNT samples (Figure S1). Qualitative assessment of the dispersion and settling characteristics of the various MWNT samples (Figure S2). Mass loss curves from thermo-gravimetric analysis (TGA) of MWNT samples (Figure S3). Representative images of cells stained with DAPI and PI (Figure S4). Summary of fluorescence-based toxicity assays following *E. coli* cell contact with MWNT-coated filters (Figure S5). Percent increase in concentration of RNA in the supernatant of cells incubated with MWNT samples compared to that of the control (Figure S6). This material is available free of charge via the Internet at <http://pubs.acs.org>.

### Literature Cited

- (1) Balasubramanian, K.; Burghard, M. Chemically functionalized carbon nanotubes. *Small* **2005**, *1*, 180–192.
- (2) Furtado, C. A.; Kim, U. J.; Gutierrez, H. R.; Pan, L.; Dickey, E. C.; Eklund, P. C. Debundling and dissolution of single-walled carbon nanotubes in amide solvents. *J. Am. Chem. Soc.* **2004**, *126*, 6095–6105.
- (3) Xing, Y. C.; Li, L.; Chusuei, C. C.; Hull, R. V. Sonochemical oxidation of multiwalled carbon nanotubes. *Langmuir* **2005**, *21*, 4185–4190.
- (4) Jia, G.; Wang, H. F.; Yan, L.; Wang, X.; Pei, R. J.; Yan, T.; Zhao, Y. L.; Guo, X. B. Cytotoxicity of carbon nanomaterials: Single-wall nanotube, multi-wall nanotube, and fullerene. *Environ. Sci. Technol.* **2005**, *39*, 1378–1383.
- (5) Zhu, Y.; Ran, T. C.; Li, Y. G.; Guo, J. X.; Li, W. X. Dependence of the cytotoxicity of multi-walled carbon nanotubes on the culture medium. *Nanotechnology* **2006**, *17*, 4668–4674.
- (6) Ding, L. H.; Stilwell, J.; Zhang, T. T.; Elboudwarej, O.; Jiang, H. J.; Selegue, J. P.; Cooke, P. A.; Gray, J. W.; Chen, F. Q. F. Molecular characterization of the cytotoxic mechanism of multiwall carbon nanotubes and nano-onions on human skin fibroblast. *Nano Letters* **2005**, *5*, 2448–2464.
- (7) Pulskamp, K.; Diabate, S.; Krug, H. F. Carbon nanotubes show no sign of acute toxicity but induce intracellular reactive oxygen species in dependence on contaminants. *Toxicol. Lett.* **2007**, *168*, 58–74.
- (8) Magrez, A.; Kasas, S.; Salicio, V.; Pasquier, N.; Seo, J. W.; Celio, M.; Catsicas, S.; Schwaller, B.; Forro, L. Cellular toxicity of carbon-based nanomaterials. *Nano Lett* **2006**, *6*, 1121–1125.
- (9) Wick, P.; Manser, P.; Limbach, L. K.; Dettlaff-Weglowska, U.; Krumeich, F.; Roth, S.; Stark, W. J.; Bruinink, A. The degree and kind of agglomeration affect carbon nanotube cytotoxicity. *Toxicol. Lett.* **2007**, *168*, 121–131.
- (10) Sayes, C. M.; Liang, F.; Hudson, J. L.; Mendez, J.; Guo, W. H.; Beach, J. M.; Moore, V. C.; Doyle, C. D.; West, J. L.; Billups, W. E.; Ausman, K. D.; Colvin, V. L. Functionalization density dependence of single-walled carbon nanotubes cytotoxicity in vitro. *Toxicol. Lett.* **2006**, *161*, 135–142.
- (11) Tian, F. R.; Cui, D. X.; Schwarz, H.; Estrada, G. G.; Kobayashi, H. Cytotoxicity of single-wall carbon nanotubes on human fibroblasts. *Toxicol. in Vitro* **2006**, *20*, 1202–1212.
- (12) Saxena, R. K. A. W.; Mcgee, J. K.; Daniels, M. J.; Boykin, E.; Gilmour, I. Enhanced in vitro and in vivo toxicity of poly-dispersed acid-functionalized single-wall carbon nanotubes. *Nanotoxicology* **2007**, *1*, 291–300.
- (13) Delhaes, P.; Couzi, M.; Trinquecoste, M.; Dentzer, J.; Hamidou, H.; Vix-Guterl, C. A comparison between Raman spectroscopy and surface characterizations of multiwall carbon nanotubes. *Carbon* **2006**, *44*, 3005–3013.
- (14) Kang, S.; Herzberg, M.; Rodrigues, D. F.; Elimelech, M. Antibacterial Effects of Carbon Nanotubes: Size Does Matter! *Langmuir* **2008**, *24*, 6409–6413.
- (15) Kang, S.; Pinault, M.; Pfefferle, L. D.; Elimelech, M. Single-walled carbon nanotubes exhibit strong antimicrobial activity. *Langmuir* **2007**, *23*, 8670–8673.
- (16) Nguyen, T. H.; Elimelech, M. Adsorption of plasmid DNA to a natural organic matter-coated silica surface: Kinetics, conformation, and reversibility. *Langmuir* **2007**, *23*, 3273–3279.
- (17) Olmsted, S. B.; Erlandsen, S. L.; Dunny, G. M.; Wells, C. L. High-Resolution Visualization by Field-Emission Scanning Electron-Microscopy of Enterococcus-Faecalis Surface-Proteins Encoded by the Pheromone-Inducible Conjugative Plasmid Pcf10. *J. Bacteriol.* **1993**, *175*, 6229–6237.
- (18) Bom, D.; Andrews, R.; Jacques, D.; Anthony, J.; Chen, B. L.; Meier, M. S.; Selegue, J. P. Thermogravimetric analysis of the oxidation of multiwalled carbon nanotubes: Evidence for the role of defect sites in carbon nanotube chemistry. *Nano Letters* **2002**, *2*, 615–619.
- (19) Garcia, D.; Manas, P.; Gomez, N.; Raso, J.; Pagan, R. Biosynthetic requirements for the repair of sublethal membrane damage in *Escherichia coli* cells after pulsed electric fields. *J. Appl. Microbiol.* **2006**, *100*, 428–435.
- (20) Pantarotto, D.; Singh, R.; McCarthy, D.; Erhardt, M.; Briand, J. P.; Prato, M.; Kostarelos, K.; Bianco, A. Functionalized carbon nanotubes for plasmid DNA gene delivery. *Angew. Chem. Int. Ed.* **2004**, *43*, 5242–5246.
- (21) Shvedova, A. A.; Castranova, V.; Kisin, E. R.; Schwegler-Berry, D.; Murray, A. R.; Gandelsman, V. Z.; Maynard, A.; Baron, P. Exposure to carbon nanotube material: Assessment of nanotube cytotoxicity using human keratinocyte cells. *J Toxicol. Environ. Health A* **2003**, *66*, 1909–1926.
- (22) Shvedova, A. A.; Kisin, E. R.; Mercer, R.; Murray, A. R.; Johnson, V. J.; Potapovich, A. I.; Tyurina, Y. Y.; Gorelik, O.; Arepalli, S.; Schwegler-Berry, D.; Hubbs, A. F.; Antonini, J.; Evans, D. E.; Ku, B. K.; Ramsey, D.; Maynard, A.; Kagan, V. E.; Castranova, V.; Baron, P. Unusual inflammatory and fibrogenic pulmonary responses to single-walled carbon nanotubes in mice. *Am J Physiol-Lung C* **2005**, *289*, L698–L708.

ES8010173